New Insights into Charge Flow Processes and Their Impact on the Activation of Ethene and Ethyne by Cu(I) and Ag(I) Sites in MFI

ARTICLE *in* THE JOURNAL OF PHYSICAL CHEMISTRY C · MAY 2010

Impact Factor: 4.77 · DOI: 10.1021/jp1002676

5 AUTHORS, INCLUDING:

Ewa Broclawik
Polish Academy of Sciences
153 PUBLICATIONS **1,484** CITATIONS
SEE PROFILE

Pawel Kozyra
Jagiellonian University
42 PUBLICATIONS **333** CITATIONS
SEE PROFILE

Mariusz Mitoraj
Jagiellonian University
54 PUBLICATIONS **1,174** CITATIONS
SEE PROFILE

New Insights into Charge Flow Processes and Their Impact on the Activation of Ethene and Ethyne by Cu(I) and Ag(I) Sites in MFI

E. Broclawik,*,† J. Załucka,‡ P. Kozyra,‡ M. Mitoraj,‡ and J. Datka‡

Institute of Catalysis, Polish Academy of Sciences, ul. Niezapominajek 8, 30-239 Kraków, Poland, and Faculty of Chemistry, Jagiellonian University, ul. Ingardena 3, 30-060 Kraków, Poland

Received: January 11, 2010; Revised Manuscript Received: April 14, 2010

This paper concerns the activation of ethene and ethyne molecules on two cationic sites (Cu(I) and Ag(I)) in ZSM-5 zeolite. QM/MM calculations were carried out to obtain geometric structure and vibrational frequencies. A novel analysis tool, NOCV (natural orbitals for chemical valence) supported by an ETS energy decomposition scheme, was applied to characterize charge flow between adsorbed molecules and the cationic site in ZSM-5 zeolite. The ETS-NOCV method allows for separating independent components of differential electron density into donation and backdonation channels, responsible for the substrate activation. It also helps to evaluate the importance of particular density transfer channels in the activation process. Two partition schemes into two subsystems are proposed here to extract complete information on the electronic balance between the molecule, the cation, and the zeolite framework. Both cationic sites (Cu(I) and Ag(I)) and both molecules (ethene and ethyne) are compared and the differences in the red-shift of CC stretching frequency are rationalized in terms of donation and backdonation charge transfer processes. They are shown to depend as well on metal specific properties as on the interaction between the metal and the framework.

Introduction

Zeolites are a group of compounds of great importance for science as well as for industry. They are used as catalysts in such processes as cracking, alkylation, and polymerization. Both natural and synthetic zeolites are used also as sorbents and ion exchangers. Zeolites with transition metal ions in exchangeable positions are of special significance. Such cationic sites are catalytically active in denox and other redox reactions. Our earlier IR studies and DFT quantum chemical calculations evidenced that Cu(I) ions in zeolites CuZSM-5, CuX, or CuY and also in CuMCM-41 material were able to activate multiple bonds in organic molecules such as alkenes (ethene, propene, and butenes), ethyne, benzene, acetone, and formaldehyde.[1] This activation was evidenced by significant red-shift of the IR multiple bond stretching frequency. High activity of copper sites toward NO or alkenes, promoted by their ability to donate electrons to π antibonding orbitals of the adsorbate, is well-known both from experiment and theoretical modeling.[1−5] Our former IR studies showed that silver sites in zeolites did also activate multiple bonds in organic molecules, similarly to copper ions; however, this effect for Ag was smaller than for Cu ions: the red-shifts of IR bands of stretching of multiple bonds for the Ag site was about half of the value observed for the Cu site.[6] Thus in this study Cu(I) sites are examined parallel with Ag(I) ones to disclose factors essential for high activity of copper sites in MFI zeolite.

Ethene is of interest here as it forms complexes with various cationic centers, where the C═C bond can be either shortened or elongated, depending not only on the cation but also on its next neighbors.[7] It is used in many industrial processes like production of propene over Ag(I) exchanged zeolites,[8] production of aromatic compounds[9] and oxygenated compounds,[10] and production of isoprene and methacrylic acid used in polymer synthesis.[11] Molecules with triple C≡C bond have also wide range of application in many processes, e.g., Diels−Alder reaction,[12] di- and oligomerization,[7,13] Reppe's cycle,[14] and synthesis of N-nonsubstituted 1,2,3-triazols.[15] Ethyne is a good representative of this group. In many processes ethene and ethyne undergo transformations along similar reaction mechanisms, involving preliminary activation of the CC bond. Moreover, ethene and ethyne are good candidates for probe molecules to examine zeolite properties: they are small and highly symmetric and exhibit large effects while interacting with a center, such as geometry changes and IR frequency shifts (significant especially for ethyne).[1,6,16−19]

Coinage metal cations, bare or coordinated by selected model ligands, have already been studied in the context of their interaction with alkene or alkyne molecules by several groups, including theoretical and/or experimental researches (see, e.g., refs 20−23 and references therein). Electron rich molecules like ethene and ethyne form complexes with cationic sites where they are good electron donors to the central ion (e.g., Cu(I) or Ag(I)) as well as good electron acceptors. Both of these processes are important for activation, but π-backdonation is believed to be crucial in the case of molecules with multiple bonds.[1,21,23−26] For the purpose of quantitative estimation of donation and backdonation effects energy decomposition schemes are very often used.[27−29] This is achieved by the decomposition of the orbital interaction term into different irreducible representations. However, for molecules with no symmetry, such approaches hardly provide separate information on donation and backdonation processes.

Along this line, our work presents the first screening application of the recently proposed tool for charge flow decomposition, invoked to discriminate Cu and Ag cations embedded in a realistic model of the MFI framework. To this end, the widely accepted mechanism for adsorbed molecule activation by donation and backdonation is examined by means

* Corresponding author. E-mail: broclawi@chemia.uj.edu.pl.
† Polish Academy of Sciences.
‡ Jagiellonian University.

10.1021/jp1002676
Published on Web 05/07/2010

of a novel quantum chemical tool for theoretical analysis of electron density deformation upon bond formation, ETS-NOCV.[30] It is based on natural orbitals for chemical valence (NOCV) combined with extended transition state method (ETS) and is here for the first time successfully applied to critically differentiate various cationic sites in zeolites and their interaction with ethene and ethyne. In ETS-NOCV analysis, two partition schemes are proposed to extract complete information on the electronic balance between the molecule, the cation, and the zeolite framework. The role of zeolitic framework in promoting site activity is highlighted and clarified in a joint analysis of complementary pictures of electron density transfer between framework oxygens and the cation, accompanying donation from or backdonation to the molecule.

Methodology

Calculations. The calculations were carried out by combined quantum mechanics and molecular mechanics methods (QM/MM). In this scheme the selected part of the system, containing adsorbed molecule, cationic center and its nearest neighborhood, is treated with quantum chemical accuracy while the rest of the framework is treated with less computationally demanding molecular mechanics with periodic boundary conditions. The Turbomole package[31] was applied at the QM level and the Gulp code[32] in MM part, both linked via QMPot program.[33] The QMPot program is a variation of the QM/MM method designed for zeolites. Density functional theory (DFT) was used as the QM method with the hybrid potential B3LYP[34] for geometry optimization and frequencies. Calculated frequencies were referred to experimental values measured at room temperature. For selected properties gradient potential PBE[35] has been used for comparative purposes. Our previous experience showed that for bonding energy PBE potential is closer to experiment while for frequencies B3LYP seems to be more reliable.[17] Both potentials were applied with triple-ζ basis set. In classical part of calculations core−shell model potential[36] was used with the parametrization from papers by Sauer and Sierka for Si, Al, O, and H atoms[37] and Nachtigallová et al. for Cu(I) ion.[38] The interactions between hydrocarbon molecule and zeolite framework at MM level were represented by electrostatic interactions, with charges +0.1 on hydrocarbon H atoms and −0.2 or −0.1 on C atoms (for ethene and ethyne respectively); dispersion interactions with zeolite O atoms were described by Lennard-Jones potential with parameters from ref.[39] The bonding within the molecule and between metal ion and ethene/ethyne was described only at QM level.

After QMPot optimization, single-point calculations with ADF software (PBE potential) were performed to apply NOCV analysis (vide infra) and to obtain bond orders[40] and Hirshfeld charges.[41] The charge flow between predefined fragments of the systems of interest has been studied based on recently proposed natural orbitals for chemical valence method (NOCV)[42,43] combined with the Ziegler-Rauk energy decomposition scheme (ETS, extended transition state).[27,44] ETS-NOCV allows us to separate and quantitatively estimate the electron charge transfer channels. It was shown[42,43] that the natural orbitals for chemical valence pairs (Ψ_{-k},Ψ_k) decompose the differential density $\Delta\rho$ into NOCV-contributions $(\Delta\rho_k)$

$$\Delta\rho(r) = \sum_{k=1}^{M/2} \upsilon_k[-\psi_{-k}^2(r) + \psi_k^2(r)] = \sum_{k=1}^{M/2} \Delta\rho_k(r) \quad (1)$$

where ν_k and M stand for the NOCV eigenvalues and the number of basis functions, respectively. Visual inspection of deformation density plots $(\Delta\rho_k)$ helps to attribute symmetry and the direction of the charge flow. In addition, these pictures are enriched by providing the energetic estimations, $\Delta E_{orb}(k)$, for each $\Delta\rho_k$ within ETS-NOCV scheme.[30] The exact formula which links ETS and NOCV method will be given in the next paragraph, after we briefly discuss the basic concept of ETS scheme. In this method total bonding energy ΔE_{bond} between interacting fragments is divided into three components. The first component, ΔE_{dist}, referred to as the distortion term, represents the amount of energy required to promote the separated fragments from their equilibrium geometry to the structure they will take up in the combined molecule. The second term, ΔE_{steric}, corresponds to the steric interaction between fragments. It accounts for Pauli repulsion contribution together with the electrostatic term. Finally, the last stabilizing term, ΔE_{orb}, represents the interactions between the occupied molecular orbitals of one fragment with the unoccupied molecular orbitals of the other fragment as well as mixing of occupied and virtual orbitals within the same fragment (inner-fragment polarization). This energy term may be linked to the electronic bonding effect coming from the formation of a chemical bond.

In the combined ETS-NOCV scheme,[30] the orbital interaction term (ΔE_{orb}) is expressed in terms of NOCV's eigenvalues as

$$\Delta E_{orb} = \sum_k \Delta E_{orb}(k) = \sum_{k=1}^{M/2} \upsilon_k[-F_{-k,-k}^{TS} + F_{k,k}^{TS}] \quad (2)$$

where $F_{i,i}^{TS}$ are diagonal Kohn−Sham matrix elements defined over NOCV with respect to the transition state (TS) density (at the midpoint between density of the molecule and the sum of fragment densities). This term gives the energetic measure for $\Delta\rho_k$ that may be related to the importance of a particular electron flow channel for the bonding between fragments and its consequences.

Models. In the present study, the M7 cluster (cutoff the wall in the main channel), the metal cation, and alkene or alkyne molecule are treated with quantum chemical accuracy and the rest of the framework is treated by molecular mechanics. The M7 cluster is a fragment of the ZSM-5 framework containing a 6-membered ring made of two consolidated 5-membered rings. M stands for "main channel", and 7 stands for 7 Si or Al atoms. Our model has one Al atom as the ZSM-5 zeolite is of low aluminum content and is electroneutral. To saturate peripheral bonds in the model, silicon atoms from the next coordination sphere are replaced by hydrogen atoms. Cu(I) or Ag(I) has been placed in the middle of the 6-membered ring and the hydrocarbon molecule over the cation (toward the main channel). Figure 1 shows an example of the elementary cell containing the M7 cluster hosting Cu(I) with adsorbed ethyne (part treated by QM in bold). In the final geometry optimized for ZSM-5, the metal cation (with a hydrocarbon molecule bound by two carbons) is coordinated only to two oxygen atoms belonging to the same AlO_4 tetrahedron (see Figure 1). Other three structures (Ag(I)/ethene/ethyne, Cu(I)/ethene, not shown separately) are similar. The model used in this work is analogous to that described by Rejmak et al. in ref 17.

QM cluster (optimized at QMPot level) was subjected to NOCV analysis in order to extract the information on the electron density rearrangement upon the bond formation. In ADF calculations, the cluster geometry was not reoptimized since we believe that combined QM/MM calculations better reproduce the structure embedded in the zeolite framework than free cluster optimization. In order to analyze electron density transfer

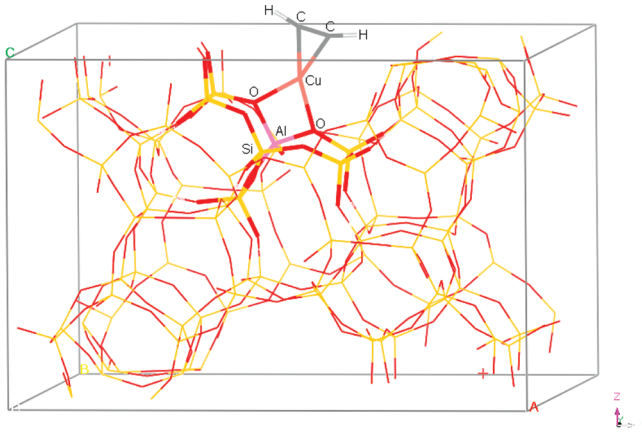

Figure 1. Periodic element containing Cu(I) cationic site in M7 cluster with adsorbed ethyne, embedded in ZSM-5 framework (fragment treated by QM in bold).

TABLE 1: Bonding Energies, Changes in C═C Bond Lengths and Bond Orders, and Frequency Shifts for Ethene Interacting with Metal Sites in ZSM-5

	ΔE_{bond}/kcal·mol^{-1} B3LYP/PBE	ΔR_{CC}/Å	Δb.o.	$\Delta\nu_{calc}$[a]/cm^{-1} B3LYP/PBE	$\Delta\nu_{exp}$[a]/cm^{-1}
Cu(I)	−31.1/−38.4	0.048	−0.43	−104/−128	−85
Ag(I)	−16.4/−23.5	0.037	−0.30	−79/−105	−41

[a] All frequency shifts are related to absolute values for ethene in gas phase: 1623 (exp[59]), 1691 (B3LYP), and 1643 (PBE).

processes we apply two types of fragmentation of the adsorption system into subsystems. The natural way of the partition of the system composed of an adsorbed molecule (Mol) and a site (M7-M(I)) is the one denoted here as [Mol]//[M(I)-M7]. This decomposition scheme describes the charge flow between the cationic center and the molecule. In addition, we consider the alternative division, denoted as [Mol-M(I)]//[M7], where a molecule and a cation stand for one subsystem, and a zeolite framework stands for the other. This partition scheme should bring more specific information on the charge flow between the cation and the zeolite framework. The NOCV method with both partition schemes was described and used previously in the analysis of benzene adsorption on Cu(I) and Ag(I) sites in ZSM-5[45,46] and ethene interacting with CuY.[17]

Results

Ethene. Geometry optimization for adsorption of ethene on the copper or silver cation centers gives the structure with ethene adsorbed side-on allowing for efficient interaction of the C═C π-electron system with the cation. Due to d−π overlap, Cu(I) and Ag(I) sites interact much stronger with ethene than sodium site recalled here as a reference. The total interaction energy, ΔE_{bond} (Table 1), is calculated as the difference between the energy of the composed system and the sum of energies of noninteracting fragments. PBE bonding energy calculated in this study is by 40% larger for copper site (−38.4 kcal/mol) than for silver one (−23.5 kcal/mol). The interaction between ethene and either the silver[47−49] or copper cation[22,47,49] has already been modeled with various methods. Regardless of the method, the total bonding energy between ethene and free cations is always lower for silver than for copper by a dozen or so kcal/mol (in absolute values). Depending on the method, ΔE_{bond} falls between −44 and −57 kcal/mol for Cu^+ and between −30 and −40 kcal/mol for Ag^+. The experimental value of ethene bonding with Ag^+ (−34 kcal/mol[50]) agrees with the calculated results. Moreover, some research has also been done on the interaction of ethene with copper sites in FAU or MFI zeolites.[17,18] According to these data, the Cu(I) coordinated by oxygen atoms belonging to the same tetrahedron exhibits ΔE_{bond} in the range between −34 and −37 kcal/mol for the B3LYP potential[17,18] and −46 kcal/mol for PBE.[17] Clearly, the presence of a zeolite framework decreases the interaction energy with respect to free cation. On the other hand, very low interaction energy between Na^+ site in zeolite and ethene (ca. −5.5 kcal/mol, at physisorption level) conforms to the already widely accepted opinion that the electronic interaction between the transition metal and the adsorbate is more pronounced compared to nontransition metals and determines specificity of the bonding.[23,26] In this spirit, the ability of transition-metal exchanged cations to adsorb selectively molecules is frequently attributed through the Dewar−Chatt−Duncanson model of bonding[51] to the "π-complexation mechanism". Based on quantum chemical methods, the formation of adducts would result in strong interaction stemming from the donation of bonding π electrons of adsorbed molecule to the s(d_{z^2}) orbital of the metal (via σ-channel) and the so-called d−π* backdonation from d orbital of the metal to antibonding π* orbitals of the molecule.[26] Thus electronic properties of the metal site (in particular its ability to donate or accept electrons) strongly contribute to the selective adsorption and prospective activation of the molecule. In addition to total interaction energy, changes of other specific quantities are related to the extent of the interaction and, what follows, activation of ethene. One of the quantities which can be used as the indirect measure of the activation is the elongation of the C═C bond, amounting to 0.048 Å for copper and 0.037 Å for silver site. It goes in line with the change of bond order with respect to the free molecule (Table 1): −0.43 and −0.30 for the copper and silver sites, respectively. The activation of ethene, evidenced already by the C═C bond elongation, results obviously in the weakening of the carbon−carbon bond; the strength of the C═C bond has a direct reflection on the frequency lowering of the stretching vibration (discussed further in details). Our IR measurements yield the red-shift for the C═C bond of 85 cm^{-1} for Cu(I) and 41 cm^{-1} for Ag(I) site in ZSM5, respectively, compared to free molecule.[52]

Hübner et al. measured IR frequency of the C═C bond in ethene adsorbed on Cu(I) exchanged FAU zeolite being red-shifted by 80 or 90 cm^{-1} with respect to free molecule, depending on the site type.[18] This is in good agreement with the present work and with previous findings of our group for Cu(I) sites in X or Y faujasites.[53] The effect of frequency red-shift originating from the [M(η^2-C_2H_4)]$^+$ interaction was also found in complexes containing Ag cations coordinated by various ligands.[54−57] The data presented in these works for silver complexes gives the IR red-shifts in the narrow range of 41−51 cm^{-1}.[54−57]

Stretching C═C vibration is no more symmetry forbidden in IR spectroscopy, as the ethene molecule is distorted upon adsorption and symmetry restrictions are released. The average dihedral angle between C═C and the H−C−H plane decreases from 180° to 165° and 169° for Cu(I) and Ag(I) sites, respectively. Calculated frequencies, though overestimated with respect to experiment (see Table 1), also give a red-shift bigger for the copper site than for the silver one: 104 and 85 cm^{-1}, respectively (B3LYP). Similar overestimation of calculated red-shifts was also obtained in earlier works on ethene adsorbed on copper sites in zeolites[1,17,18] and on bare silver cations.[48] The larger error in the red-shift calculated by the PBE potential for silver can be explained by the gradient potentials tendency to

TABLE 2: Results of Hirshfeld Population Analysis: Total Charges on Ethene, Metal Cation, and Zeolite Fragment before and after Adsorption on Cu(I) and Ag(I) Sites in ZSM-5

	Cu(I) M7		Ag(I) M7	
	before/after	ΔQ	before/after	ΔQ
ethene	0	+0.019	0	+0.056
	+0.019		+0.056	
M(I)	+0.364	+0.078	+0.480	+0.007
	+0.442		+0.487	
M7	−0.364	−0.097	−0.480	−0.062
	−0.461		−0.542	

lose accuracy with increasing nuclear charge of atoms in a given complex;[58] this tendency was already discussed for Ag^+ interacting with ethene molecule and ascribed partly to relativistic effects.[20] Nonetheless, in the following sections, we concentrate on the rationalization of relative changes in IR shifts caused by ethene adsorption on various cationic sites thus we hope that inaccuracies in absolute frequency shifts should not obscure the final conclusions.

Charge Flow Analysis. One of the indicators of charge flow is the change in the charges extracted from population analysis. The results of population analysis condensed to fragments, given in Table 2, indicate already noticeable differences between electronic interaction of ethene with Cu(I) or Ag(I) sites. The neutral ethene molecule becomes positive upon adsorption on both kinds of sites, but for copper site positive charge of ethene is much smaller than for silver, presumably due to the stronger backdonation. Simultaneously, copper transfers more electrons to the framework than it gains from the molecule whereas silver cation preserves almost the same charge. In both cases, the zeolite framework stores negative charge. However, the resultant charge flow provided by population analysis condensed to fragments perceives solely net electron density outflow from ethene to the site while the backdonation process is still hidden behind.

Since the final charge on the fragment apparently depends on the balance between the two contradictory charge flow processes (donation and backdonation), NOCV analysis has been invoked to resolve differential charge density into specific channels and to quantitatively discriminate the two processes. The contributions to orbital interaction energy attributed to particular channels of the electron density flow ("NOCV-resolved" ETS energy analysis) delivered information about their share in the covalent component of the binding between the fragments. In Figures 2−5 the charge flow channels with $\Delta E_{orb}(i)$ contributions bigger in absolute values than 4 kcal/mol are shown (blue, gain of electrons; red, loss of electrons). We have found strictly two leading density flow channels in all cases, with other contributions by 1 order of magnitude less important.

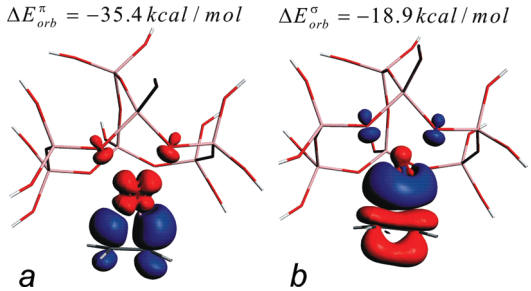

Figure 2. Predominant contributions ($|\Delta E_{orb}| > 4$ kcal/mol) to differential electron density for $[C_2H_4]$//[Cu(I)-M7] fragmentation. Blue, gain of electron density; red, loss of electron density.

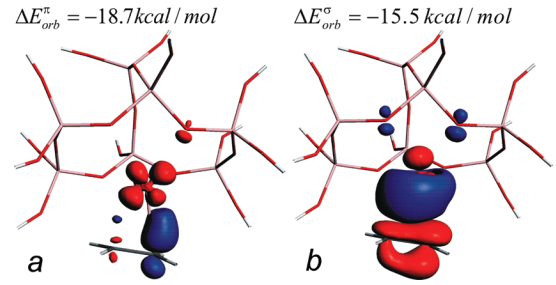

Figure 3. Predominant contributions to differential electron density for $[C_2H_4]$//[Ag(I)-M7] fragmentation. Blue, gain of electron density; red, loss of electron density.

Figures 2 and 3 show charge flows between cationic site and the ethene molecule (for $[C_2H_4]$//[M(I)-M7] partition) for the copper and silver sites, respectively. For the copper site, the biggest contribution to the orbital interaction energy (−35.4 kcal/mol) corresponds to the backdonation from the copper d orbital to the antibonding ethene orbital, aided by some electron density transfer from the framework oxygens. (Figure 2a). This channel illustrates clearly the d−π* backdonation mechanism.[26] The second channel visualizes the process of electron density transfer from the occupied π ethene orbital to the empty copper orbital (exhibiting s(d) character) and further to framework oxygens (Figure 2b). This channel corresponds to the σ-donation component of the π-complexation interaction. Both these phenomena weaken the C═C bond. The differential density for the interaction between ethene and the silver site is also composed of two significant contributions, analogous to those for a copper site. However, the increment to orbital interaction energy for π-backdonation (Figure 3a) is two times smaller for silver than for the copper site; orbital energy contribution for the donation (from ethene π orbital to copper s orbital, Figure 3b) is less sensitive to the metal (−18.9 kcal/mol vs −15.5 kcal/mol for Cu(I) and Ag(I), respectively).

It should be pointed out that the nature of the M(I)-C_2H_4 interaction (M = Cu, Ag) was the subject of numerous previous investigations based on various models.[20−23,48,49] In our study, however, we are focusing solely on the electronic part of the M(I)-C_2H_4 interaction, because this interaction is believed to be the most important for C═C bond activation. To this end, quantitative description of σ-donation and π-backdonation processes is presented and compared with relevant studies by other authors in Table 3. Earlier results, based either on pure ETS scheme supported by symmetry conditions or on symmetry-resolved population analysis, show that σ-donation significantly prevails over π-back-bonding[20−23,48,49] for bare cations or simple model systems. Interestingly, our ETS-NOCV results, characterizing the M(I)-C_2H_4 interaction with the participation of the zeolite framework (M7), exhibit exactly the opposite trend, i.e., π-backdonation dominates over σ-bonding, as shown in Table 3. It should be noted that similar observations on the dominant role of π-back-bonding in M(I)-C_2H_4 interaction was made by Ziegler et al. and Morokuma et al. in the case of complexes containing phosphorus ligands.[60−62,23] This evidently points to a significant role of zeolite network in controlling the M(I)-C_2H_4 interaction.

Accordingly, let us now shed some light on the interaction between the framework and a cation. Charge flow channels for the alternative way of system fragmentation ([C_2H_4-M(I)]//[M7]) are presented in Figures 4 and 5 for Cu and Ag, respectively.

For both metals only the channels supplying electrons from framework oxygens to the fragment composed of the cation with adsorbed ethene were found to be important and are presented

TABLE 3: Quantitative Estimation of σ-Donation and π-Backdonation Processes Characterizing M(I)-C_2H_4 Interactions (M = Cu, Ag)

	M7Cu(I)-C_2H_4	M7Ag(I)-C_2H_4	Cu(I)-C_2H_4	Ag(I)-C_2H_4	Cu(I)-$(C_2H_4)_2$	Ag(I)-$(C_2H_4)_2$	Ag(I)-$(C_2H_4)_3$
ref	this work[a]	this work[a]	22[b]/49[c]	22[b]/49[c]	20[b]	20[b]	48[b]
σ- donation	−18.9	−15.5	−39.9/0.188e	−30.7/0.175e	−68.5	−57.5	−39.0
π-back-donation	−35.4	−18.7	−21.5/0.066e	−8.6/0.038e	−23.0	−12.2	−7.3

[a] Contributions to orbital interaction energy defined by ETS-NOCV, kcal/mol. [b] Contributions to orbital interaction energy defined by appropriate representations, kcal/mol. [c] Population analysis, electron unit.

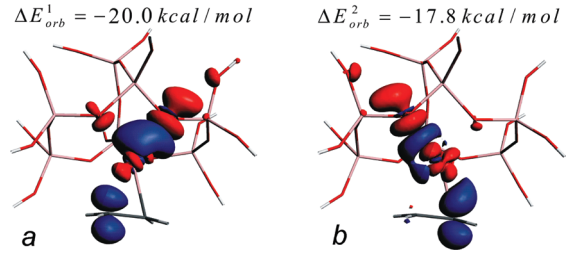

Figure 4. Predominant contributions to differential electron density for [C_2H_4-Cu(I)]//[M7] fragmentation.

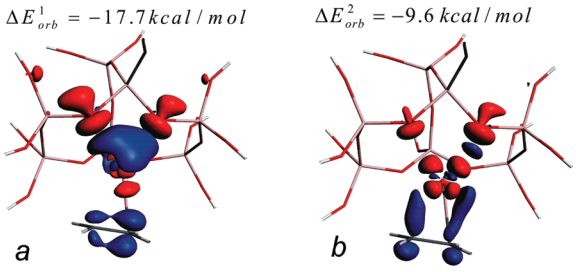

Figure 5. Predominant contributions to differential electron density for [C_2H_4-Ag(I)]//[M7] fragmentation.

here. Figure 4a and b put together describes electron density transfer to the copper and ethene molecules from the nearest oxygen atoms. In other words, partial neutralization of the cation charge by the framework enhances backdonation to the molecule, identified in Figure 2a. Joint analysis of the processes depicted in Figure 2a together with Figure 4, panels a and b, clearly shows the mediation of copper cation in supplying ethene with electrons by framework oxygen atoms which clarifies as well the participation of the surrounding zeolite lattice in electron density transfer and in the process of ethene activation as the role of the cation. Analogous reasoning can be carried out for the silver site on the basis on Figures 3a and 5a,b, but the interaction between silver cation and the framework is apparently less efficient for promoting backdonation than that for copper: the sum of $\Delta E_{orb}(i)$ in Figure 5a,b for [C_2H_4-Ag(I)]//[M7] partition (−27.3 kcal/mol) is 30% lower than the analogous one for copper (−37.8 kcal/mol). The energetic measure for π-backdonation from the cation to ethene is 50% higher for copper than for silver (compare Table 7); accordingly, the difference in the interaction with lattice oxygens explains about 60% of the variation between copper and silver sites with respect to their activation ability toward ethene.

Ethyne. Theoretical modeling shows that qualitatively ethyne interacts with both cationic sites in the same way as ethene. CH≡CH approaches as well Cu^+ and Ag^+ cations as Ag(I) and Cu(I) sites in a side-on arrangement with one of the π bonds interacting with metal d orbitals. The interaction between Cu^+ or Ag^+ cations and ethyne has already been studied by other authors,[21,47,63−65] and, in line with ethene, the copper cation was shown to interact more strongly with ethyne than the silver one; absolute values of ΔE_{bond} were found to be ca. 12 kcal/mol larger for Cu^+ than for Ag^+ cation.

TABLE 4: Bonding Energies, Changes in C≡C Bond Lengths and Bond Orders, and Frequency Shifts for Ethyne Interacting with Metal Sites in ZSM-5

	ΔE_{bond} /kcal·mol^{-1} B3LYP/PBE	ΔR_{CC} [Å]	Δb.o.	$\Delta\nu_{calc}$[a]/cm^{-1} B3LYP/PBE	$\Delta\nu_{exp}$[a]/cm^{-1}
Cu(I)	−28.5/−35.0	0.033	−0.42	−175/−203	−161
Ag(I)	−11.8/−17.1	0.020	−0.28	−122/−167	−60[b]

[a] All frequency shifts are related to absolute values for ethyne molecule in gas phase: 1974 (exp.[59]), 2071 (B3LYP), and 2010 (PBE). [b] Experimental frequency measured at 250 K is 1918 cm^{-1} (shift of −56 cm^{-1}); the shift given in the table and discussed in the text corresponds to room temperature and is estimated.

Binding energies calculated by us (PBE and B3LYP) for ethyne interacting with the M(I)-M7 sites in MFI are by 17−18 kcal/mol bigger in absolute values for Cu(I) than for Ag(I) (Table 4). However, one should be aware that the interaction energies of the same cation can also vary by similar amount, depending on the site and/or zeolite type. The difference of 14 kcal/mol in ethyne binding energies either for SII or SIII Cu(I) sites in FAU was found in ref.[19] For the M(I)-M7 model assumed here for MFI the interaction lies in-between those calculated for SII and SIII sites in FAU. The comparison of Tables 1 and 4 shows that ethyne bonding energy is lower than that for ethene by ca. 3 kcal/mol for Cu(I) and by ca. 5 kcal/mol for the Ag(I) site. The difference in ΔE_{bond} between the two sites is slightly bigger (by 2−3 kcal/mol) for ethyne than for ethene; thus, the impact of the cation type seems to be more pronounced for ethyne than for ethene. Nevertheless, though absolute values of the C≡C bond elongation in ethyne are smaller than those for C=C bond in ethene, it is not reflected in a smaller activation. Similarly, although the comparison of overall ethyne binding energies for zeolitic sites with those for bare cations suggests that silicalite surrounding decreases the interaction energy, M(I) sites impose even stronger activation of the CC bond (vide infra).

Our QMPot modeling shows that the C≡C bond is elongated by 0.033 Å due to interaction with the copper site whereas only by 0.020 Å for silver site, which goes in line with the calculated decrease of bond orders (−0.42 and −0.28 for Cu(I) and Ag(I) respectively). Ethyne looses symmetry, similarly to the case of ethene: the average angle between C≡C and C−H bonds decreases from 180° to 163° or 168° (for the Cu(I) or Ag(I) site, respectively). As a consequence, initially symmetric C≡C stretching is no longer symmetry forbidden in IR spectroscopy. Indeed, upon ethyne adsorption, the bands corresponding to C≡C vibration appear in the IR spectrum at 1813 cm^{-1} for the Cu(I) site[16] and at 1908 cm^{-1} for the Ag(I) site (see footnote in Table 4, unpublished data). They are red-shifted by 161 and 60 cm^{-1}, accordingly, with respect to the gas phase[59] which indicates more pronounced activation in the case of the copper site. Hübner et al.[19] have reported similar IR red-shifts of the C≡C vibration (by 142−161 cm^{-1}) for copper sites in FAU zeolite. Nonzeolitic silver species are also known to weaken the C≡C bond to the same extent as zeolitic sites. Reisinger et al. have measured the red-shift of 60 cm^{-1} for ethyne adsorbed

TABLE 5: Results of Hirshfeld Population Analysis: Total Charges on Ethyne, Metal Cation, and Zeolite Fragment before and after Adsorption on Cu(I) and Ag(I) Sites in ZSM-5

	Cu(I) M7		Ag(I) M7	
	before/after	ΔQ	before/after	ΔQ
ethyne	0	+0.043	0	+0.107
	+0.043		+0.107	
M(I)	+0.364	+0.067	+0.480	0.000
	+0.431		+0.480	
M7	−0.364	−0.109	−0.480	−0.107
	−0.473		−0.587	

on Ag^+ coordinated by organic ligands,[21] whereas for HC≡CPh interacting with $[HB(3,5\text{-}(CF_3)_2Pz)_3]Ag^+$, a red shift of 69 cm^{-1} was reported.[66] The overall comparison of experimental red-shifts reported for Cu(I) and Ag(I) moieties shows that ethyne is more sensitive to the type of the cation than ethene (differences of ca. 100 cm^{-1} versus 45 cm^{-1}).

The C≡C stretching frequency calculated by us for copper with B3LYP potential is red-shifted by 175 cm^{-1}, in good agreement with the experimental value (Table 4). Hübner et al.[19] calculated similar values for ethyne adsorbed on Cu in Y zeolite (182 cm^{-1}). Calculated red-shifts are significantly smaller for silver than for copper; however, in accord with the ethene case the difference between these red-shifts is underestimated by calculations with respect to the experimental value (assumingly due to larger overestimation of the red-shift calculated for both molecules interacting with Ag(I) site).

Charge Flow Analysis. The picture given by the population analysis for the systems with ethyne (Table 5) resembles that for ethene: it includes the information solely on the effective charge shifts and NOCV analysis is needed to extract separate channels of electron density flow. The changes of calculated fragment charges show that neutral ethyne molecule effectively looses electrons while adsorbed on a cationic site; accordingly, copper cation becomes more positive upon ethyne adsorption while the silver does not change population and the framework effectively collects electrons. Thus, also in this case the population analysis depicts only net electron density outflow from ethyne while the backdonation cannot be addressed directly, as opposed to NOCV picture already derived for ethene interacting with both cationic sites.

The detailed description of the nature of M(I)-C_2H_2 interaction (for M = Cu, Ag) was previously reported for both bare cations.[23,64,67] In addition, more complicated $[Ag(\eta^2\text{-}C_2H_2)_n]^+$ (n = 1, 3, 4) cations stabilized by $[Al(OR)_4]^-$ anions have been found experimentally, and their bonding characteristics were determined based on calculated AIM data.[21] Especially deep analysis and discussion was invoked to understand the relative importance of electrostatic and donor/acceptor nature of M(I)-C_2H_2 interaction.[68,69] In our study we are discussing solely the electronic processes, as they seem crucial in CC bond activation. It turns out that for the simplest model, involving a bare M^+ cation and a C_2H_2 molecule, π-backdonation is rather negligible when compared to σ-donation.[64] On the contrary, in planar complexes containing phosphorus ligands the M(I)-C_2H_2 interaction is characterized by very strong π-bonding, with minor stabilization stemming from σ-donation.[23,60,61] Similarly, Reisinger et al. also found the local charge depletions in the valence density of the Ag for $[Ag(\eta^2\text{-}C_2H_2)_n]^+$ (n = 1, 3, 4) cations, which was attributed to the ligand ← Ag π-backdonation.[21] Unfortunately, the authors were unable to provide quantitative estimation of either σ-contribution or π-back-bonding based on AIM data. In our study, ETS-NOCV results obtained for M(I)-C_2H_2 interaction with the participation of the zeolite framework (M7), revealed that π-backdonation dominates over σ-bonding, as seen from Figures 6 and 7. This again points at an important role of zeolite network in determining the character of M(I)-C_2H_2 interaction. Therefore, in the next paragraphs the interaction between the zeolite framework and the cation will be discussed in more detail based on ETS-NOCV scheme.

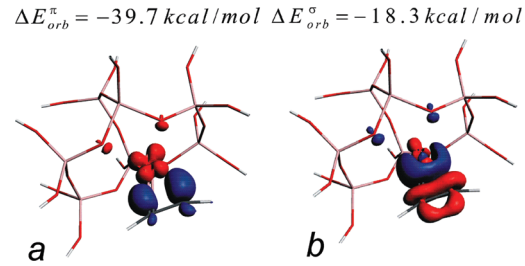

Figure 6. Predominant contributions to differential electron density for $[C_2H_2]$//[Cu(I)-M7] fragmentation.

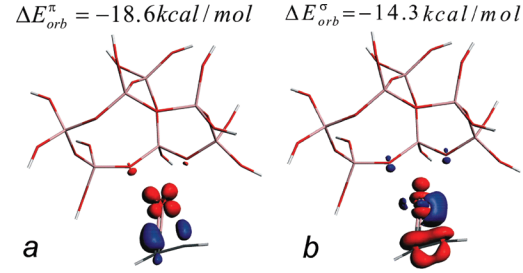

Figure 7. Predominant contributions to differential electron density for $[C_2H_2]$//[Ag(I)-M7] fragmentation.

A picture given by NOCV analysis and its discussion is analogous to that for ethene. Again, there are only two significant contributions to differential density for both cations and both partition schemes (Figures 6−9). Within the first partition scheme ($[C_2H_2]$//[Cu(I)-M7]), the most significant contribution (ΔE^{π}_{orb} = −39.7 kcal/mol) corresponds to a π-backdonation from copper cation to ethyne molecule (Figure 6a). The next one, with ΔE^{σ}_{orb} of −18.3 kcal/mol, depicts an outflow of the electron density from ethyne molecule to the cation and from the cation to the zeolite framework, attributable to σ-donation (Figure 6b). Analogous pictures for silver site (Figure 7) visualize contributions similar to the channels obtained for copper case. However, π-backdonation channel for silver (ΔE^{π}_{orb} = −18.6 kcal/mol) brings here over 50% smaller contribution to the orbital interaction energy than that for copper site; the contributions from σ-donation (Figures 6b and 7b) differ merely by ca. 4 kcal/mol.

It is worth noticing here that for copper site the significant difference is noted for π-backdonation between ethyne and ethene molecules while σ-donation is of similar importance for both molecules; for silver site both channels are of similar importance for ethene and ethyne. This seems to suggest that copper discriminates the two molecules better than silver.

The contributions to differential density for $[C_2H_2{-}Cu(I)]$// [M7] subsystems are shown in Figure 8. Once again, there are only two significant flows due to ethyne adsorption and both represent charge transfer from framework oxygen atoms. Oxygen free electron pairs deliver electrons to the cation and, by the mediation of the cation, to ethyne molecule. Figure 9 shows the contributions to differential density for $[C_2H_2{-}Ag(I)]$// [M7] division, qualitatively comparable to those for copper site but the sum of contributions to orbital interaction energy (−27.6

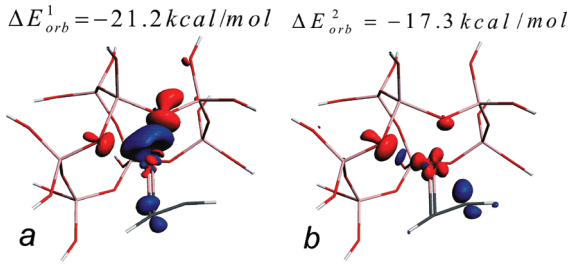

Figure 8. Predominant contributions to differential electron density for [C_2H_2-Cu(I)]//[M7] fragmentation.

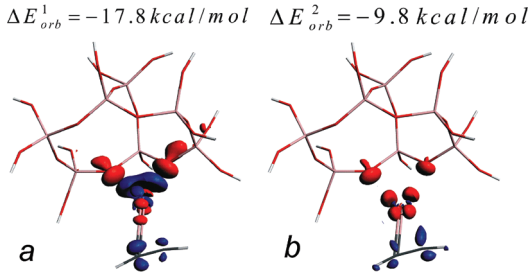

Figure 9. Predominant contributions to differential electron density for [C_2H_2-Ag(I)]//[M7] fragmentation.

TABLE 6: Selected Bond Lengths in Optimized Structures of Ethene/Ethyne Adsorbed on Cu(I) and Ag(I) Sites in ZM-5

		R(M-O) [Å]		*R*(M-C) [Å]		*R*(C−C) [Å]
C_2H_4	Cu(I)	2.044	2.085	2.042	2.031	1.372
	Ag(I)	2.303	2.340	2.269	2.244	1.361
C_2H_2	Cu(I)	2.046	2.078	1.983	1.989	1.230
	Ag(I)	2.308	2.364	2.245	2.243	1.219

kcal/mol) is by 30% lower than the analogous one for copper (−38.5 kcal/mol, Figure 8). This suggests that the influence of the framework is stronger in the case of copper than silver.

Discussion

Selected bond lengths are gathered for the two molecules and the two cations in Table 6. Coordination of both cations to lattice oxygen atoms after ethene adsorption is very similar to that for ethyne. The M-C distances are also comparable for the same metal and different hydrocarbons - ethene and ethyne. Regarding the two M(I) centers, copper is closer as well to lattice oxygen atoms as to carbon atoms than silver. Compared to the calculated geometry in gase phase (*R*(C═C) = 1.325 Å, *R*(C≡C) = 1.197 Å), the CC bonds are elongated. The CC bond elongation found in this work for ethene (0.036 and 0.047 Å for Ag(I) and Cu(I), respectively) fits well with that estimated from our calculated frequency shifts on the basis of the nonlinear dependency between calculated bond frequency decrease ($\Delta\nu$) and bond elongation (Δd) found by Reisinger et al. for BP86 potential[48] ($\Delta\nu$ of 79 and 104 cm^{-1} yield Δd of 0.030 and 0.044 Å, respectively). Nonlinear character of $\Delta\nu$ versus Δd dependency found in this work, in line with that presented in ref 48 indicates again that geometrical parameters alone do not fully reflect bond weakening measured by stretching frequency shift.

For the first division pattern, [Mol]//[M(I)-M7], the sum of orbital contributions to interaction energies for copper systems is bigger than that for silver by ca. 20 kcal/mol in the case of ethene or by ca. 25 kcal/mol for ethyne (see Table 7). This variation is predominantly due to the difference in the contributions from the π-backdonation channel. For the second partition scheme, [Mol-M(I)]//[M7], for both metals only the channels

TABLE 7: Orbital Energy Contributions Corresponding to Distinct Electron Density Flow Channels for [Mol]// [M(I)-M7] Fragmentation

		$\Delta E_{orb}(i)$ [kcal/mol]		
description		π-backdonation	σ-donation	$\Sigma\Delta E_{orb}(i)$ [kcal/mol]
C_2H_4	Cu	−35.4	−18.9	−54.3
	Ag	−18.7	−15.5	−34.2
	Δ	−16.7	−3.4	−20.1
C_2H_2	Cu	−39.7	−18.3	−58.0
	Ag	−18.6	−14.3	−32.9
	Δ	−21.1	−4.0	−25.1

TABLE 8: Orbital Energy Contributions Corresponding to Distinct Electron Density Flow Channels for [Mol-M(I)]//M7] Fragmentation

description		$\Sigma\Delta E_{orb}(i)$ [kcal/mol] supporting π-backdonation
C_2H_4	Cu	−37.8
	Ag	−27.3
	Δ	−10.5
C_2H_2	Cu	−38.5
	Ag	−27.6
	Δ	−10.9

supplying electrons from framework oxygens to the fragment composed of the cation with adsorbed molecule show up as the significant contributions. This seems to suggest that the outflow of electrons from the (already negative) framework via the cation to the adsorbate is separated from the electron inflow to the framework which may take place at the initial stage of adsorption-induced cation withdrawal from the lattice. Indeed, the comparison of the previously reported coordination of copper cation by lattice oxygens before and after adsorption of ethene,[17] indicates significant weakening of the cation-oxygen bonding after molecule sorption.

The sum of ΔE_{orb} contributions to orbital interaction energy between the cation and the framework is by ca. 10 kcal/mol bigger for copper than for the silver site as well for ethene as for ethyne (see Table 8). This shows that electronic interaction with framework oxygens is by 30% more effective for copper than for silver sites, regardless of the molecule (ethene or ethyne) which suggests that this interaction is not sensitive to the sorption of small hydrocarbon molecule with multiple bonds. This observation is supported as well by geometric properties of adsorption system (Table 6) as by analysis of contributions to orbital interaction energy (rows 3 and 6 in Table 8). However, with respect to the differences between metal cations, ethyne is more sensitive to intrinsic metal properties than ethene. Thus the analysis of the importance of the charge flow to or from the molecule, together with that between the metal ion and the framework, indicates that the efficiency of electronic interaction between the site and the molecule depends both on the cation and on its relationship with the framework and may vary among different types of molecules. In other words, the difference in the activation ability toward a given substrate between the two metal sites may be explained in part by intrinsic differences between Cu(I) and Ag(I) whereas the rest of variance should be attributed to the difference in the metal-framework interaction. From this point of view copper turned out to be more efficient than silver in both respects which explains its relatively higher activation ability.

Let us turn to the effect of the electron transfer between the site and the molecule on the C═C or C≡C bond. Backdonation from Cu(I) to the molecule is energetically by ca. 4 kcal/mol more significant for ethyne (Figure 6a) than for ethene (Figure 2a). The remaining channels are comparable (difference of at

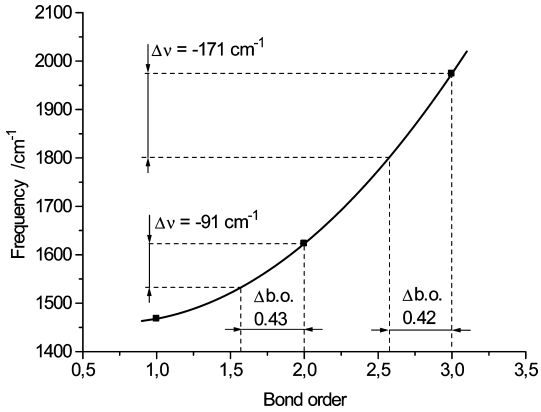

Figure 10. Dependence of experimental stretching CC bond frequency on formal bond order for free ethane, ethene, and ethyne molecules.

most 1 kcal/mol) for both hydrocarbons. Hence total orbital interaction energies also do not differ significantly with respect to the type of CC bond (the largest deviation is 5 kcal/mol for [Mol]//[Cu(I)-M7] fragmention). The changes of C═C and C≡C bond orders are also close to each other: 0.43, 0.42 for copper and 0.30, 0.28 for silver. However, the IR red-shifts for ethyne are much bigger than those for ethene as evidenced both by experiment and by calculation. Yet we must additionally take into consideration that the bonds to be activated are of significantly different strength and one should not expect similar response to the same stimulus when applied to various receptors. Prompted by the nonlinear dependence found between calculated bond elongation and stretching frequency shifts[48] for a series of $[M(I)(\eta^2\text{-}C_2H_4)_n]$ complexes, we have constructed similar plot for the direct dependence between IR frequency and formal bond order in a series of C_2 hydrocarbons with different types of CC bond. Figure 10 shows the plot of measured IR frequencies for ethane, ethene and ethyne gas phase molecules (taken from ref 59) versus their formal bond order, that is strongly related to electron density flow. It is clearly visible that the correlation is also strongly nonlinear. On the basis of the plot given in Figure 10, we can estimate the expected red-shift for copper, corresponding to the change of bond order by 0.43 for ethene with double bond, at the value of 91 cm^{-1}; similar change of bond order (by 0.42) for ethyne with triple bond would yield a much bigger IR red-shift (by 171 cm^{-1}). These two values agree perfectly with IR shifts measured for ethene and ethyne adsorbed on copper (−85 and −161 cm^{-1}, respectively). This observation clearly explains the reason why similar donation/backdonation processes lead to distinct shifts of IR frequencies in adsorbed ethene or ethyne.

Conclusions

A new type of theoretical analysis (based on natural orbitals for chemical valence, ETS-NOCV) of electron density deformation upon bond formation was for the first time successfully applied to the description of various cationic sites in MFI zeolites and their interaction with ethene and ethyne. The analysis allows for unequivocal separation of charge redistribution (accompanying molecule adsorption) into donation and backdonation processes, and assessing their energetic share in the bonding for low-symmetry systems. Moreover, energetic measures corresponding to electron flow channels give quantitative estimates of the efficiency of the cation-to-molecule π-backdonation for the bonding and activation of the molecule on the cationic site. Additional novelty of our work should follow from the joint analysis of two complementary partition schemes applied to the model of the system thought off as composed of three interacting components: hydrocarbon molecule, the Me(I) center and its closest zeolitic environment. Here, alternative analysis of electron density flow between the framework and the cation with ad-molecule shows clearly that the activation ability of the catalytic site is determined not only by intrinsic donor properties of transition metal cation but also depends to large extent on its electronic interaction with framework oxygens.

Specific conclusions inferred from the electronic structure and NOCV modeling, aided with IR experiment for Cu(I) and Ag(I) sites in MFI zeolites may be summarized as follows. Energetic measures indicate that the backdonation from the d orbital of a cation to the antibonding ethene (ethyne) orbitals brings dominant contribution to the bonding between the molecule and both cations. Combined analysis of electron flow between the molecule and the cation with that between the cation and the framework shows clearly that the ability of Cu(I) and Ag(I) to π-backdonation depends both on the cation identity and on its coordination with framework oxygens. Consequently, the framework, the metal cation and the molecule must be treated as interdependent system of joined vessels, where charge flow in one region does not leave the other parts without response. Thus the difference in the activation ability between the two metal sites may be explained in part by intrinsic differences between copper and silver cations whereas the rest of variance should be attributed to the difference in the metal-framework interaction. An electron-rich zeolite framework reinforces π-backdonation better for Cu(I) than in the case of Ag(I), which explains 60% of the predominance of Cu(I) over Ag(I) sites in the case of ethene and 50% for ethyne. On the other hand, the Cu(I) cation is a better electron donor than Ag(I) which explains the other 40% (50%) of variance in ethene (ethyne) activation. In conclusion, copper is more efficient than silver in both aspects which highly clarifies the understanding of its outstanding catalytic activity. The activation of ethene/ethyne molecule upon adsorption on cationic sites in ZSM-5 is reflected by red-shifts of IR CC stretching frequency. The match between calculated and measured differences in red-shifts provides the link between the computer modeling and IR experiment thus theoretical interpretation of the activation mechanism gains experimental support and verification.

Acknowledgment. This study was sponsored by the Ministry of Science and Higher Education (Grant Nos. N N204 1987 33 and N N204 1518 36).

References and Notes

(1) Brocławik, E.; Kozyra, P.; Datka, J. *C. R. Chim.* **2005**, *8*, 491–508.
(2) Broclawik, E.; Datka, J.; Gil, B.; Kozyra, P. *Top Catal.* **2002**, *75*, 353.
(3) Datka, J.; Brocławik, E.; Kozyra, P.; Kukulska-Zajaç, E.; Bartula, D.; Szutiak, M. *Stud. Surf. Sci. Catal.* **2004**, *154*, 2151.
(4) Datka, J.; Kozyra, P.; Kukulska-Zajaç, E.; Kobyzewa, W. *Catal. Today* **2005**, *101*, 117.
(5) Kukulska-Zajaç, E.; Kozyra, P.; Datka, J. *Appl. Catal., A* **2006**, *307*, 46.
(6) Kukulska-Zajaç, E.; Datka, J. *Microp. Mesop. Mat.* **2008**, *109*, 49–57.
(7) Tobe, M. L.; Burgess, J. *Inorg. React. Mech., Longman* **1999**, 606.
(8) Inazu, K.; Koyama, T.; Miyaji, A.; Baba, T. *J. Jpn. Petrol. Inst.* **2008**, *51*, 205.
(9) Bandiera, J.; Ben Taarit, Y. *Appl. Catal., A* **1995**, *132*, 157.
(10) (a) Asensi, M. A.; Corma, A.; Martýnez, A. *J. Catal.* **1996**, *158*, 561. (b) Xu, W.-Q.; Yin, Y.-G.; Suib, S. L.; O'Young, C.-L. *J. Catal.* **1994**, *150*, 34. (c) Houzvicka, J.; Ponec, V. *Appl. Catal., A* **1996**, *145*, 95. (d) Me'riaudau, P.; Anh, T. Vu.; Le Ngoc, H.; Naccache, C., in: Chon, H.; Ihm, S.-K.; Uh, Y. S. *Stud. Surf. Sci. Catal.* **1997**, *105*, 1373. (e) Millini,

R.; Rossini, S., in: Chon, H.; Ihm, S.-K.; Uh, Y. S. *Stud. Surf. Sci. Catal.* **1997**, *105*, 1389.
(11) Weissermel, K.; Arpe, H. J. *Ind. Org. Chem.*; Verlag Chemie: Weinheim, Germany, 1978; p 63.
(12) Sauer, J.; Sustmann, R. *Angew. Chem. Int. Ed. Engl.* **1980**, *19*, 779.
(13) (a) Gausing, W.; Wilke, G. *Angew. Chem. Int. Ed. Engl.* **1981**, *20*, 186. (b) Wilke, G. *J. Organomet. Chem.* **1980**, *200*, 349. (c) Colborn, R. E.; Vollhardt, K. P. C. *J. Am. Chem. Soc.* **1981**, *103*, 6259. (cs) Diercks, R.; Stamp, L.; Kopf, J.; Dieck, H. T. *Angew. Chem. Int. Edit. Engl.* **1984**, *23*, 893. (d) Yur'eva, L. P. *Russ. Chem, Rev.* **1974**, *43*, 48. (e) Meijer-Veldman, M. E. E.; Meijer, H. J. L. *J. Organomet. Chem.* **1984**, *260*, 199.
(14) (a) Roe, D. C.; Sheridan, R. E.; Bunel, E. E. *J. Am. Chem. Soc.* **1994**, *116*, 1163. (b) Souma, Y.; Kawasaki, H. *Catal. Today* **1997**, *36*, 91.
(15) (a) Chassaing, S.; Sido, A. S. S.; Alix, A.; Kumarraja, M.; Pale, P.; Sommer, J. *Chem.—Eur. J.* **2008**, *14*, 6713. (b) Jin, T.; Kamijo, S.; Yamamoto, Y. *Eur. J. Org. Chem.* **2004**, *2004*, 3789.
(16) Datka, J.; Kukulska-Zajaç, E.; Kobyzewa, W. *Catal. Today* **2005**, *101*, 123.
(17) Rejmak, P.; Mitoraj, M.; Broclawik, E. *Phys. Chem. Chem. Phys.* **2010**, *12*, 2321.
(18) Hübner, G.; Rauhut, G.; Stoll, H.; Roduner, E. *Phys. Chem. Chem. Phys.* **2002**, *4*, 3112.
(19) Hübner, G.; Rauhut, G.; Stoll, H.; Roduner, E. *J. Phys. Chem. B* **2003**, *107*, 8568.
(20) Tai, H.-C.; Krossing, I.; Seth, M.; Deubel, D. V. *Organometallics* **2004**, *23*, 2343.
(21) Reisinger, A.; Trapp, N.; Krossing, I.; Altmannshofer, S.; Herz, V.; Presnitz, M.; Scherer, W. *Angew. Chem., Int. Ed.* **2007**, *46*, 8295.
(22) Hertwig, R. H.; Koch, W.; Schröder, D.; Schwarz, H. *J. Phys. Chem.* **1996**, *100*, 12253.
(23) Frenking, G.; Fröhlich, N. *Chem. Rev.* **2000**, *100*, 717–774.
(24) Brocławik, E.; Datka, J.; Gil, B.; Kozyra, P. *Phys. Chem. Chem. Phys.* **2000**, *2*, 401.
(25) Brocławik, E.; Datka, J.; Gil, B.; Piskorz, W.; Kozyra, P. *Top. Catal* **2000**, *11/12*, 335.
(26) Berthomieu, D.; Delahay, G. *Catal. Rev.* **2006**, *48*, 269.
(27) Ziegler, T.; Rauk, A. *Theor. Chim. Acta* **1977**, *46*, 1.
(28) Morokuma, K. *J. Chem. Phys.* **1971**, *55*, 1236.
(29) Bickelhaupt, F. M.; Baerends, E. In *J. Kohn-Sham Density Functional Theory: Predicting and Understanding Chemistry. ReViews in Computational Chemistry*; Lipkowitz, K. B., Boyd, D. B., Eds.; Wiley-VCH: New York, 2000; Vol. 15, pp 1−86.
(30) (a) Mitoraj, M.; Michalak, A.; Ziegler, T. J. *Chem. Theory Comput.* **2009**, *5*, 962. (b) Mitoraj, M.; Michalak, A.; Ziegler, T. *Organometallics* **2009**, *28*, 3727.
(31) Ahlrichs, R.; Bär, M.; Häser, M.; Horn, H.; Kölmel, C. M. *Chem. Phys. Lett.* **1989**, *162*, 165.
(32) Gale, J. D. *J. Chem. Soc., Faraday Trans.* **1997**, *93*, 629.
(33) Sierka, M.; Sauer, J. *J. Chem. Phys.* **2000**, *112*, 6983.
(34) (a) Becke, A. D. *Phys. Rev. A* **1988**, *38*, 3098. (b) Lee, C.; Yang, W.; Parr, R. G. *Phys. Rev. B* **1998**, *37*, 785. (c) Becke, A. D. *J. Chem. Phys.* **1993**, *98*, 5648.
(35) Perdew, J. P.; Burke, K.; Ernzerhof, M. *Phys. Rev. Lett.* **1996**, *77*, 3865.
(36) Dick, B. G.; Overhauser, A. W. *Phys. Rev.* **1958**, *112*, 90.
(37) Sierka, M.; Sauer, J. *Faraday Discuss.* **1997**, *106*, 41.
(38) Nachtigallová, D.; Nachtigall, P.; Sierka, M.; Sauer, J. *Phys. Chem. Chem. Phys.* **1999**, *1*, 2019.
(39) De Moor, B. A.; Reyniers, M.-F.; Sierka, M.; Sauer, J.; Marin, G. B. *J. Phys. Chem. C* **2008**, *112*, 11796; supporting information.
(40) Mrozek, J.; Nalewajki, R. F.; Michalak, A. *Pol. J. Chem.* **1998**, *72*, 1779.
(41) Hirshfeld, F. L. *Theor. Chim. Acta B* **1977**, *44*, 129.
(42) (a) Mitoraj, M.; Michalak, A. *J. Mol. Model.* **2006**, *13*, 347. (b) Michalak, A.; Mitoraj, M.; Ziegler, T. *J. Phys. Chem. A* **2008**, *112*, 1933. (c) Srebro, M.; Mitoraj, M. *Organometallics* **2009**, *28*, 3650. (d) Mitoraj, M.; Michalak, A. *J. Mol. Model.* **2008**, *14*, 681. (e) Mitoraj, M.; Zhu, H.; Michalak, A.; Ziegler, T. *Int. J. Quantum Chem.* **2008**, DOI: 10.1002/qua.21910.
(43) Mitoraj, M.; Michalak, A. *Organometallics* **2007**, *26*, 6576.
(44) Ziegler, T.; Rauk, A. *Inorg. Chem.* **1979**, *18*, 1755.
(45) Załucka, J.; Kozyra, P.; Mitoraj, M.; Brocławik, E.; Datka, J. *Pol. J. Chem.* **2008**, *81*, 1802.
(46) Załucka, J.; Kozyra, P.; Mitoraj, M.; Brocławik, E.; Datka, J. *Stud. Surf. Sci. Catal.* **2008**, *174A*, 709.
(47) Böhme, M.; Wagener, T.; Frenking, G. *J. Organomet. Chem.* **1996**, *520*, 31.
(48) Reisinger, S.; Trapp, N.; Knapp, C.; Himmel, D.; Breher, F.; Rüegger, H.; Krossing, I. *Chem.—Eur. J.* **2009**, *15*, 9505.
(49) Kim, C. K.; Lee, K. A.; Kim, C. K.; Lee, B.-S.; Lee, H. W. *Chem. Phys. Let.* **2004**, *391*, 321.
(50) Guo, B. C.; Castleman, A. W., Jr. *Chem. Phys. Lett.* **1991**, *181*, 16.
(51) Dewar, M. *Bull. Soc. Chim. Fr.* **1951**, C71–79. Chatt, J.; Duncanson, L. A. *J. Chem. Soc.* **1953**, 2939.
(52) Kukulska-Zajaç, E.; Datka, J. private communication.
(53) Datka, J.; Kozyra, P. *J. Mol. Struct.* **2005**, *744−747*, 991–996.
(54) Reisinger, A.; Trapp, N.; Krossing, I. *Organometallics* **2007**, *26*, 2096.
(55) Dias, H. V. R.; Wang, X. *J. Chem. Soc., Dalton Trans.* **2005**, 2985.
(56) Krossing, I.; Reisinger, A. *Angew. Chem.* **2003**, *42*, 5725.
(57) Powell, D. B.; Scott, J. G. V.; Sheppard, N. *Spectrochim. Acta* **1972**, *28*, 327.
(58) Engel, E. Orbital-Dependent Functionals for the Exchange-Correlation Energy: A Third Generation of Density Functionals. In *A Primer in Density Functional Theory*; Fiolhais, C., Nogueira, F., Marques, M., Eds.; Springer-Verlag: Berlin, 2003; p 59.
(59) Shimanouchi, T. *Tables of Molecular Vibrational Frequencies, Consolidated Vol. I*; NSRDS National Bureau of Standards: Gaithersberg, MD, 1972; Vol. 39, pp 1−160; http://webbook.nist.gov/chemistry/.
(60) Ziegler, T. *Inorg. Chem.* **1985**, *24*, 1547.
(61) Li, J.; Schreckenbach, G.; Ziegler, T. *Inorg. Chem.* **1995**, *34*, 3245.
(62) Kitaura, K.; Sakaki, S.; Morokuma, K. *Inorg. Chem.* **1981**, *20*, 2292.
(63) Sodupe, M.; Bauschlicher, C. W. *J. Phys. Chem.* **1991**, *95*, 8640.
(64) Miralles-Sabater, J.; Merchán, M.; Nebot-Gil, I.; Viruela-Martin, P. M. *J. Phys. Chem.* **1988**, *92*, 4853.
(65) Tsipis, A. C. *Organometallics* **2010**, *29*, 354–363.
(66) Dias, H. V. R.; Wang, Z.; Jin, W. *Inorg. Chem.* **1997**, *36*, 6205.
(67) Pidun, U.; Frenking, G. *J. Organomet. Chem.* **1996**, *525*, 269.
(68) Krapp, A.; Frenking, G. *Angew. Chem., Int. Ed.* **2008**, *47*, 7796.
(69) Himmel, D.; Trapp, N.; Krossing, I.; Altmannshofer, S.; Herz, V.; Eickerling, G.; Scherer, W. *Angew. Chem., Int. Ed.* **2008**, *47*, 7798.

JP1002676